CHAPTER IV

MIMO CHANNEL UNDER PRACTICAL CONDITIONS

In practical channel conditions, due to an increased number of parameters, the knowledge of the CSI at the transmitter may never perfect. The effects of imperfect CSI at the receiver in a SISO system were studied in [83] and the work is extended in [98] to a MISO system with imperfect channel estimation and quantized feedback with no delays in a block fading channel. Other works considering similar problems, for example [99], [82], [85] and [100], have concentrated mainly on imperfect channel estimation at the receiver without any feedback. However, it is important to note again that all the works mentioned above presumed an iid channel matrix. For that reason, the analysis of MIMO systems on channel capacity and / or the BER with imperfect CSI at both the transmitter and the receiver in a spatially correlated Rayleigh fading channel are the next main inspective problem.

Typically, CSI is provided to the transmitter through the CSI feedback for Frequency Division Duplexing (FDD) systems or by channel reciprocity for Time Division Duplexing (TDD) systems. In both cases, the estimated CSI is imperfect due to estimation errors and feedback delay.

In this chapter, the information theoretic aspects of Spatial Multiplexing MIMO Zero Forcing receiving (SM-MIMO-ZF) system operating under practical channel conditions will be covered. Lower bounds of the mutual information for the SM-MIMO-ZF system will be derived, and followed by determination of the BER of that system.

4.1 System Definition and Channel Modeling

First of all, consider an MIMO system with N_T transmitter antennas and N_R receiver antennas, where assume that $N_R \geq N_T$, as shown in Figure 4.1. The incoming data stream is first split into N_T data sub-streams with the same symbol rate 1/T (T is

the symbol period), which are independently encoded and modulated. Also, assume the same modulation scheme M is used for each data sub-stream and all the transmitters are operating at the same carrier frequency. In addition, data transmission is organized into bursts of L symbols and the modulated signals are radiated through the respective antennas.

Consider the structure of the equivalent baseband systems of a single-user link. Assume that the transmitted signals encounter Rayleigh flat fading before reaching the receiver antennas. The MIMO channel is modeled and can be denoted by a complex matrix $\mathbf{H} \in \mathbb{C}^{N_R \times N_T}$ with zero mean, unit variance and complex Gaussian entries. The received data vector $\mathrm{r} \in \mathbb{C}^{N_R \times 1}$ at a time instance is expressed in the complex baseband vector as follows

$$\begin{aligned} \mathrm{r} &= \mathbf{HF}\mathrm{s}+\mathrm{n} \\ &= \hat{\mathbf{H}}\mathbf{F}\mathrm{s}+\left(\mathbf{H}-\hat{\mathbf{H}}\right)\mathbf{F}\mathrm{s}+\mathrm{n} \\ &= \hat{\mathbf{H}}\mathbf{F}\mathrm{s}+\hat{\mathrm{n}} \end{aligned} \tag{4.1}$$

where

- $\mathbf{F}$ is the $\left(N_R \times N_T\right)$ precoding matrix used for power link adaptation,
- $\mathrm{s} \in \mathbb{C}^{N_T \times 1}$ denotes the transmitted vector,
- $\mathrm{n} \in \mathbb{C}^{N_R \times 1}$ is an Additive White Gaussian Noise (AWGN) vector with zero mean and variance σ_n^2,
- $\hat{\mathrm{n}}=\left(\mathbf{H}-\hat{\mathbf{H}}\right)\mathbf{F}\mathrm{s}+\mathrm{n}$ is the additional effective noise plus interference.

The channel and noise variance is normalized in such way that the entries of $\mathbf{H}$ and n have unit variance. We also assume that both the channel fading process and the noise process have no correlation between time instances.

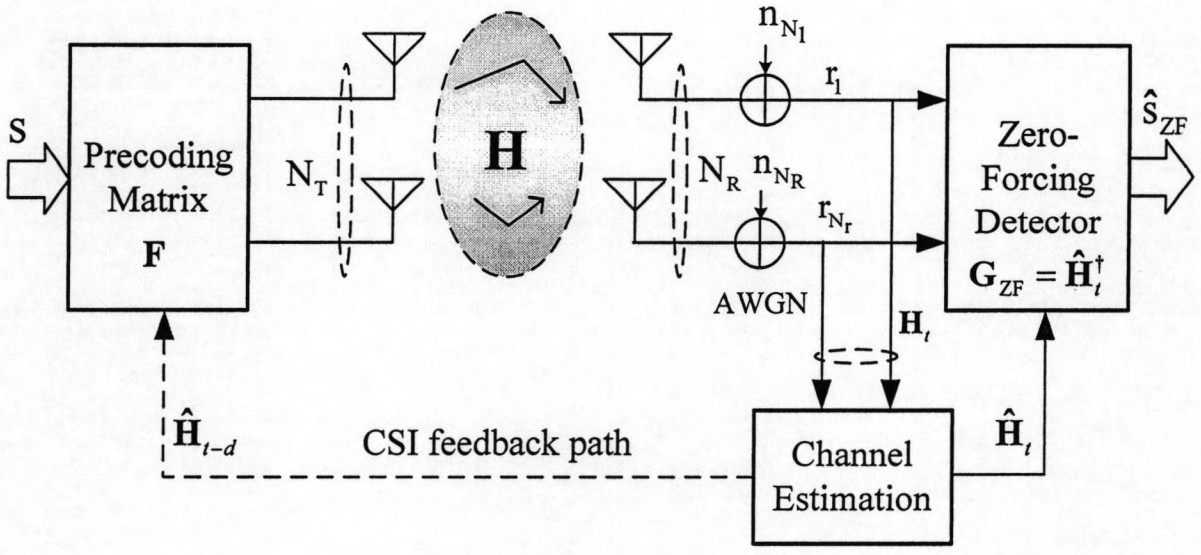

Figure 4.1 Block diagram of the proposed SM-MIMO-ZF system

4.1.1 Channel Model with Estimation Error

In practice, as previously mentioned the channel estimation errors occur at the receiver, denote $\hat{\mathbf{H}}$ as the estimated channel of $\mathbf{H}$ at the receiver. Therefore, the channel matrix can be re-modeled as follows

$$\mathbf{H} = \hat{\mathbf{H}} + \mathbf{E} \tag{4.2}$$

where

- $\mathbf{E} \in \mathbb{C}^{N_r \times N_t}$ is the channel estimation error matrix (is also known as deviation of the estimated channel to the true channel) that is uncorrelated with $\hat{\mathbf{H}}$ and each element is also iid with complex Gaussian random variables independent of $\mathbf{H}$.

$$\mathbf{E} \in CN\left(0, \sigma_e^2\right) \tag{4.3}$$

- σ_e^2 represents the quality of the channel estimation which is assumed to be known at both the transmitter and the receiver

$$\sigma_e^2 = \text{MMSE} = \mathrm{E}\left(\mathbf{H}_{ij}^2\right) - \mathrm{E}\left(\hat{\mathbf{H}}_{ij}^2\right) = \frac{E\left[\left|h_{ij} - \hat{h}_{ij}\right|^2\right]}{E\left[\left|h_{ij}\right|^2\right]} \tag{4.4}$$

- P_s is the total power that subject to a total transmit power constrain P_s for fulfilling as follows,

$$\mathrm{tr}\left(\mathbf{F}\mathbf{F}^H\right) = \sum_{k=1}^{\nu} \lambda_k^2 = P_s \tag{4.5}$$

with $\nu = \min\left(N_T, N_R\right)$.

- $\mathbf{F}$ is the optimal structure of the precoder matrix and is given by

$$\mathbf{F} = \mathbf{U}\boldsymbol{\Lambda}, \tag{4.6}$$

with $\mathbf{U}: (\nu \times \nu)$ is the unitary matrix, and the diagonal power allocation matrix is $\boldsymbol{\Lambda} = diag\left[\sqrt{\lambda_1}, \ldots, \sqrt{\lambda_\nu}\right]$ (4.7)

Normalization ensures that the total expected transmitted power is independent of N_T for a fixed P_s. At the receiver side, since we are considering the spatial multiplexing MIMO system with reliable feedback channel with delays, the quantized power adaptation matrix $\hat{P} = diag(\hat{p}_1, \ldots, \hat{p}_v)$ in a global power constraint in such $\mathrm{tr}(\hat{P}) = P_s$.

4.1.2 Spatial Correlation Coefficient

The channel estimation error described in the previous subsection is characterized by the correlation coefficient between the true and the estimated channels. Define the correlation coefficient between the true channel gain and its estimation as given by

$$\rho = \frac{E\left[h_{ij}\hat{h}_{ij}^{*}\right]}{\sqrt{E\left[\left|h_{ij}\right|^2\right] \cdot E\left[\left|\hat{h}_{ij}\right|^2\right]}} = \sqrt{1-\sigma_e^2}, \tag{4.8}$$

where

- $h_{ij}, \hat{h}_{ij}$ represent the $(i,j)^{th}$ element of $\mathbf{H}$, and $\hat{\mathbf{H}}$, respectively.

Eq. (4.8) represents the range of $\sigma_e^2 \in [0,1]$ and it is a measure of the accuracy of the channel estimation. The value $\sigma_e^2 = 0$ indicates that there is no estimation error.

A particular channel estimator is the sample average of pilot or training transmission in flat fading channel. This estimator is both unbiased and computational efficient. As the power of the pilot symbols and the number of pilot symbols increase. The channel estimator becomes more accurate in term of MMSE [103]. The correlation coefficient approaches to 1 means that the channel estimator becomes more accurate.

In addition, the channel time correlation ρ is a function of the maximum Doppler and the time lag between when channel is estimated and it is used for precoding design (see Figure 4.2). Here is the proposal expression using the standard

Bessel function based on Jakes spectrum for ρ which assumes uniformly distributed scatters on a circle around the antenna:

$$\rho \triangleq \frac{E\left[h_{ij}(t_0)h_{ij}^{*}(t_0+\Delta t)\right]}{\sigma_{ij}^2}$$
$$= J_0\left(2\pi f_d \Delta t\right), \tag{4.9}$$

where

- $J_0(\cdot)$ is the zero-*th* order Bessel function of the first kind,
- f_d is the maximum Doppler spread,
- Δt is the time delay which is the time difference between the estimation of the channel and the time at which the transmission occurs channel estimation error matrix (is also known as deviation).

From (4.9), obviously ρ is a function of the Doppler frequency and feedback delay. Jakes' model is used for the discussion here in a time selective narrowband channel because of its simplicity and popularity. However, any generic model can be used to suit the temporal and spatial characteristics of a specified channel.

In the next Subsections, the other important factors, which affect the reliability of the CSI will discuss:

- Quality of channel estimation,
- Delayed feedback transmission.

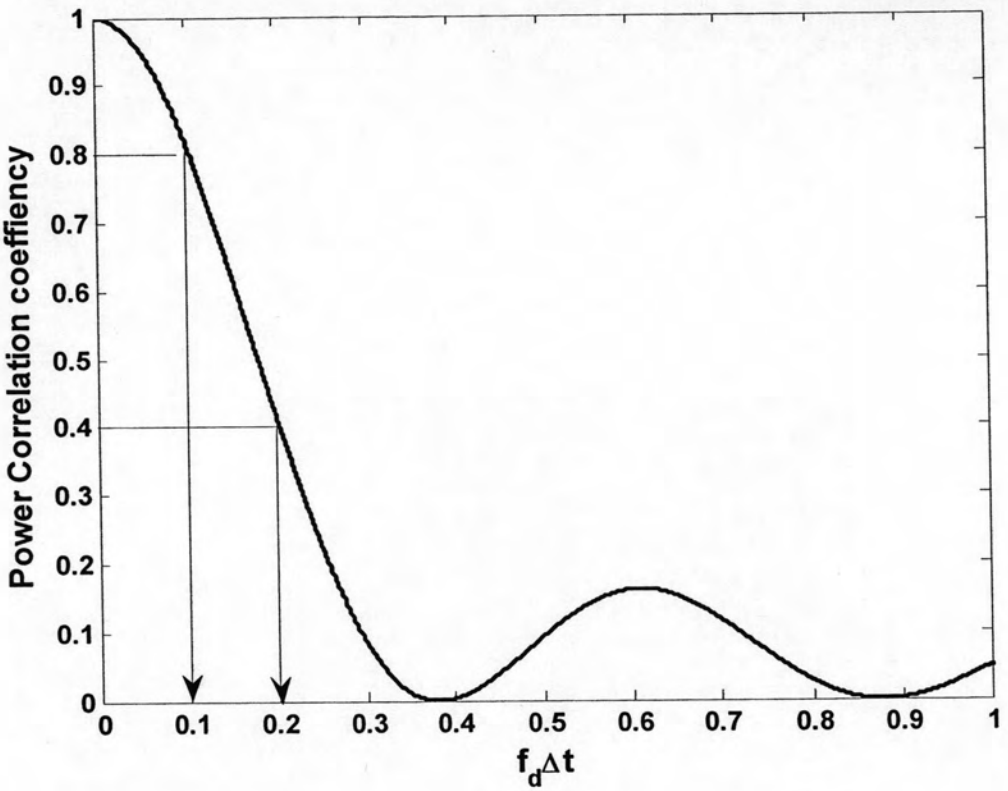

Figure 4.2 Power correlation coefficiency as functions of the Doppler spread and time lag

4.1.3 Quality of Channel Estimation

In section 4.1.1, at the time instant t, consider $\mathbf{H}_t = \hat{\mathbf{H}}_t + \mathbf{E}_t$, where $\hat{\mathbf{H}}_t$ is the channel estimation error matrix and $\mathbf{E}_t \in \mathbb{C}^{N_R \times N_T}$ is its estimation error at discrete-time index. The two terms are uncorrelated, and each entry is Zero-Mean Circularly Symmetric Complex Gaussian (ZMCSCG) with variance of σ_e^2, which dictates the quality of the channel estimation.

Here, the most straightforward method is Zero Forcing (ZF) scheme which uses for channel estimation due to its simplicity of matrix inversion at the receiver (however noted that, in spite of its simplicity, the analysis is complicated due to the perturbation of the channel matrix). The channel estimation error σ_e^2 in continuous fading channels is caused by both noise and time varying channels. The variance can be expressed as

$$\sigma_e^2 \triangleq \mathrm{E}\left[\left\|\mathbf{H} - \hat{\mathbf{H}}\right\|_{\mathrm{F}}^2\right] \tag{4.10}$$

4.1.4 Delayed Feedback Transmission

The delay of feedback transmission depends mostly on the distance between the transmitter side and the receiver side and thus in time-variant. The CSI is estimated at the receiver and sent back to the transmitter via a feedback channel. Thus, feedback delay and overhead, processing delay and practical constraints on modulation, coding, and antenna selection must be taken into accounts. Assume at time index t, there is a discrete-time difference Δt between the actual channel matrix $\mathbf{H}_t$ and the delayed feedback matrix $\mathbf{H}_{t-d}$ at time instant $(t-d)$, where both of them are error-free. Deviation between them is denoted by

$$\mathbf{D}_t = \mathbf{H}_t - \mathbf{H}_{t-d} \tag{4.11}$$

The entries of $\mathbf{D}_t$ denote as complex Gaussian variables with variance σ_d^2.

The difference between the true channel matrix and its feedback value at the discrete time index t is

$$\begin{aligned}\boldsymbol{\Delta}_t &= \mathbf{H}_t - \hat{\mathbf{H}}_{t-d} \\ &= \left(\mathbf{H}_t - \mathbf{H}_{t-d}\right) + \left(\mathbf{H}_{t-d} - \hat{\mathbf{H}}_{t-d}\right) \\ &= \mathbf{D}_t + \mathbf{E}_{t-d}\end{aligned} \tag{4.12}$$

Therefore, the entries of $\boldsymbol{\Delta}_t$ denote as complex Gaussian variables with variances of delayed feedback and estimation errors: $\sigma_\delta^2 = \sigma_d^2 + \sigma_e^2$.

4.2 Proposal Procedure of the System

The proposal procedure of the SM-MIMO-ZF system is proposed in the block diagram as below

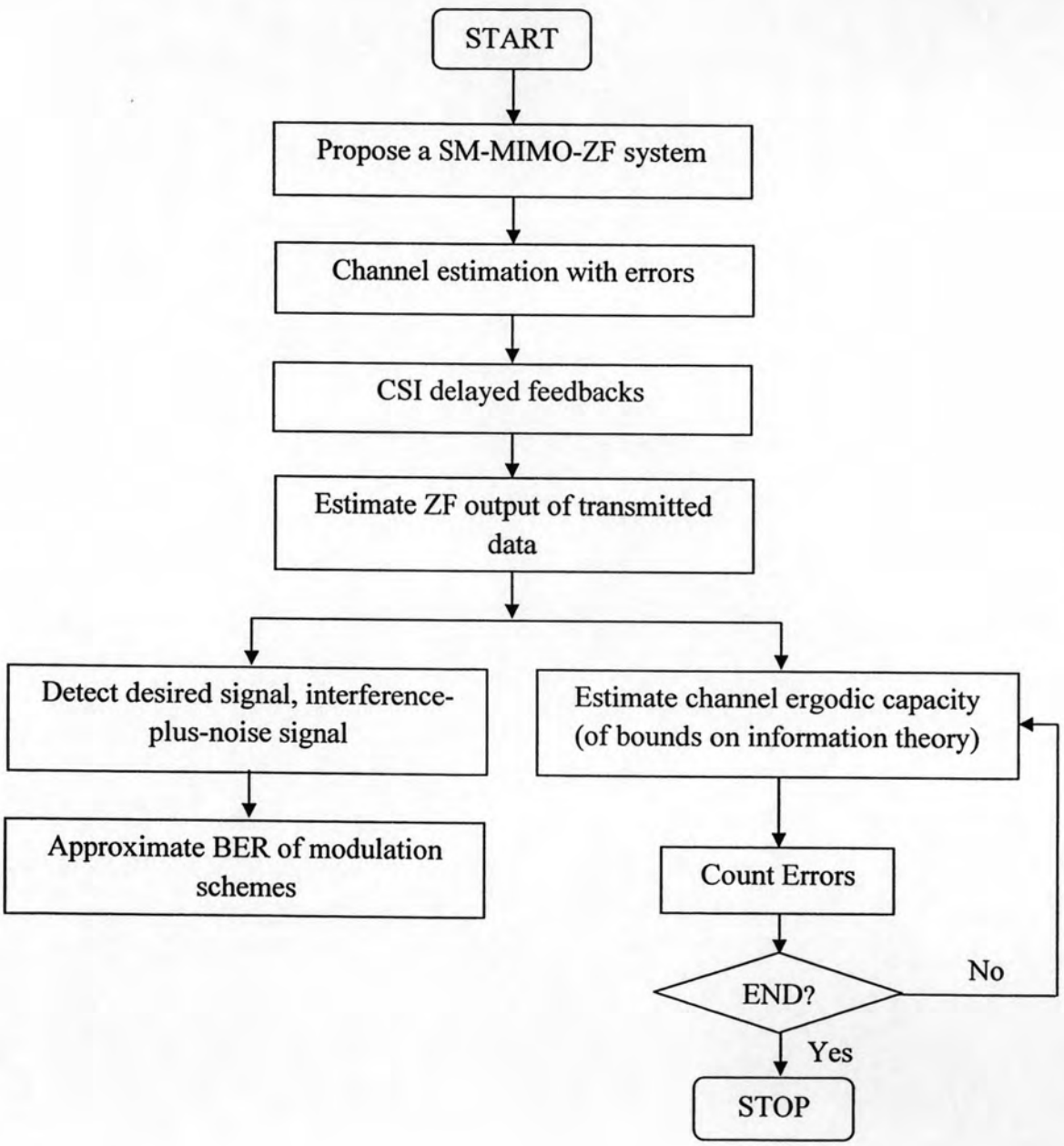

Figure 4.3 Block diagram of procedure of the proposed SM-MIMO-ZF system

4.3 Bounds on Mutual Information in Practical Conditions

An exact expression for the maximum instantaneous mutual information appears difficult to discover. Instead, the lower bounds have been derived. In this section, some results in [101], [102], and [103] is briefly presented for mutual information on MIMO system with imperfect CSI at the receiver side. Thereafter, we will present the extended study for bounds on mutual information of the proposed SM-MIMO-ZF system with channel estimation errors, delayed feedbacks to the transmitter under spatially correlation in continuous flat fading channel.

4.3.1 Imperfect CSI at the Receiver for iid Channel

In the case that perfect CSI at the receiver (Rx) and no CSI at the transmitter (Tx), it is well known that the mutual information of an MIMO system given by [15]

$$I^{\text{iid}}\left(\mathrm{s},\mathrm{r}\,|\,\mathbf{H}\right)=\log_2\det\left(\mathbf{I}_{N_\mathrm{R}}+\frac{P_s}{N_\mathrm{T}\sigma_n^2}\mathbf{H}\mathbf{H}^H\right) \tag{4.13}$$

For the case of imperfect CSI at the Rx and no CSI at the Tx, the lower bound for the instantaneous mutual information were extended in [83] to multiple antennas at the both Tx and Rx:

$$I^{\text{iid}}\left(\mathrm{s},\mathrm{r}\,|\,\mathbf{H}\right)\geq I_{\text{lb}}^{\text{iid}}\left(\mathrm{s},\mathrm{r}\,|\,\hat{\mathbf{H}}\right),$$

$$I_{\text{lb}}^{\text{iid}}\left(\mathrm{s},\mathrm{r}\,|\,\hat{\mathbf{H}}\right)=\log_2\left(\det\left(\mathbf{I}_{N_\mathrm{R}}+\frac{P_s}{2N_\mathrm{T}\sigma_n^2}\frac{2\sigma_n^2}{2\sigma_n^2+P_s\sigma_e^2}\hat{\mathbf{H}}\hat{\mathbf{H}}^H\right)\right) \tag{4.14}$$

$$=\log_2\left(\det\left(\mathbf{I}_{N_\mathrm{R}}+\frac{P_s}{2N_\mathrm{T}\sigma_n^2}\frac{2\sigma_n^2}{2\sigma_n^2+P_s\sigma_e^2}\hat{\mathbf{S}}\right)\right),$$

where

- $\hat{\mathbf{S}} = \hat{\mathbf{H}}\hat{\mathbf{H}}^H$ has a Wishart distribution of the estimated channel matrix

In addition, the lower bound on mutual information for imperfect CSI at Rx and no CSI at Tx can be expressed as follows

$$I_{\text{lb}}^{\text{iid}}\left(\text{s},\text{r}\,|\,\hat{\mathbf{H}}\right) = \sum_{k=1}^{\nu} \log_2\left(1 + \frac{P_s}{N_T}\frac{\hat{\lambda}_k}{\frac{P_s}{2}\frac{\sigma_e^2}{\sigma_n^2}+1}\right), \tag{4.15}$$

with $\nu = \min\left(N_{\text{T}}, N_{\text{R}}\right)$, and $\hat{\lambda}_k\,(k = 1,\ldots,\nu)$ is the unordered eigenvalues of a Wishart matrix $\hat{\mathbf{S}}$.

When the rank of $\hat{\mathbf{H}}$ is ν, P_s is the total power at the Tx and the ergodic channel capacity is performed by expectation over the distribution of the eigenvalues $\left\{\hat{\lambda}_k\right\}$ of $\hat{\mathbf{S}}$

$$C_{\text{lb}}^{\text{iid}} = E_{\hat{\mathbf{H}}}\left\{C_{\text{lb}}^{\text{iid}}\left(P_s,\hat{\mathbf{H}}\right)\right\};\;\; C_{\text{lb}}^{\text{iid}}\left(P_s,\hat{\mathbf{H}}\right) = \max_{E\left(\text{s}^H\text{s}\right)}\left\{I_{\text{lb}}^{\text{iid}}\left(\text{s},\text{r}\,|\,\hat{\mathbf{H}}\right)\right\} \tag{4.16}$$

From (4.14) and (4.15), it is clearly shown that the imperfect CSI at the Rx degrades the effective SNR due to the reason of an increase in the variance of noise process by $P_s\sigma_e^2$. The ergodic channel capacity is therefore degraded.

4.3.2 Imperfect CSI at the Receiver and Delayed Feedbacks to Transmitter for Spatially Correlation Channel

The capacity of MIMO system under imperfect CSI conditions with iid channel is summarized in subsection 4.3.1. However, the preceding works are not realistic in practical conditions due to the following reasons, which are still not considered for MIMO systems:

- Delayed feedback CSI from the receiver to the transmitter, and

- Spatially correlation channel

Therefore, the above two important parameters are taken into consideration in the current study. As in the following: a lower bound for a correlated fading channel will be firstly derived, and then the effects of estimation errors on the channel gain will be included.

The lower bound for imperfect CSI at Rx in spatially correlated channel can be expressed straightforward in the following. Using the fact that conditioning always decreases the entropy: $\mathrm{h}\left(\mathrm{s}-\mathbf{G}_{\mathrm{ZF}}\mathrm{r}\,|\,\mathrm{r},\hat{\mathbf{H}}\right)\geq\mathrm{h}\left(\mathrm{s}-\mathbf{G}_{\mathrm{ZF}}\mathrm{r}\,|\,\hat{\mathbf{H}}\right)$.

$$\begin{aligned} I^{\mathrm{corr}}\left(\mathrm{s},\mathrm{r}\,|\,\hat{\mathbf{H}}\right) &= \mathrm{h}\left(\mathrm{s}\,|\,\hat{\mathbf{H}}\right)-\mathrm{h}\left(\mathrm{s}\,|\,\mathrm{r},\hat{\mathbf{H}}\right) \\ &= \mathrm{h}\left(\mathrm{s}\,|\,\hat{\mathbf{H}}\right)-\mathrm{h}\left(\mathrm{s}-\mathbf{G}_{\mathrm{ZF}}\mathrm{r}\,|\,\mathrm{r},\hat{\mathbf{H}}\right) \\ &\geq I_{\mathrm{lb}}^{\mathrm{corr}} \\ &= \mathrm{h}\left(\mathrm{s}\,|\,\hat{\mathbf{H}}\right)-\mathrm{h}\left(\mathrm{s}-\mathbf{G}_{\mathrm{ZF}}\mathrm{r}\,|\,\hat{\mathbf{H}}\right) \\ &= \log_2\left(\left|\mathbf{I}_{N_{\mathrm{R}}}+\mathbf{Z}\left(E\left[\hat{\mathrm{n}}\hat{\mathrm{n}}^{H}\,|\,\hat{\mathbf{H}}\right]+\mathbf{Z}\right)^{-1}\right|\right) \end{aligned} \tag{4.17}$$

where

- $\mathrm{h}\left(\mathrm{s}\,|\,\hat{\mathbf{H}}\right)$ is the different entropy of s conditioned on $\hat{\mathbf{H}}$.
- $\mathbf{G}_{\mathrm{ZF}}=f\left(\mathrm{r},\hat{\mathbf{H}}\right)$ is chosen to be the ZF estimator of s from r given $\hat{\mathbf{H}}$ and is employed as $\mathbf{G}_{\mathrm{ZF}}=\hat{\mathbf{H}}^{\dagger}=\mathbf{F}^{H}\mathbf{H}^{H}\left(\mathbf{H}^{H}\mathbf{F}^{H}\mathbf{F}\mathbf{H}\right)^{-1}$, where † denotes the pseudo-inverse operation.
- $\mathbf{Z}=\hat{\mathbf{H}}\hat{\mathbf{\Lambda}}\hat{\mathbf{H}}^{H},\quad \hat{\mathbf{\Lambda}}=diag\left(\lambda_1,\lambda_2,\ldots,\lambda_v\right)$ (4.18)

In spatially correlated channel matrix with ZF estimator at Rx side, with making use of Eq. (4.1) and Eq. (4.2), $E\left[\hat{\mathrm{n}}\hat{\mathrm{n}}^{H}\,|\,\mathbf{H}\right]$ can then be processed as follows

$$
\begin{aligned}
E\left[\hat{\mathbf{n}}\hat{\mathbf{n}}^H|\hat{\mathbf{H}}\right] &= E\left[\left(\mathbf{H}-\hat{\mathbf{H}}\right)\mathbf{F}\mathbf{s}\mathbf{F}^H\mathbf{s}^H\left(\mathbf{H}-\hat{\mathbf{H}}\right)^H|\hat{\mathbf{H}}\right]+\sigma_n^2\mathbf{I}_{N_\mathrm{T}} \\
&= E\left[\left(\mathbf{EF}\right)\mathbf{s}\mathbf{s}^H\left(\mathbf{EF}\right)^H|\hat{\mathbf{H}}\right]+\sigma_n^2\mathbf{I}_{N_\mathrm{T}} \\
&= \boldsymbol{\Omega}
\end{aligned}
\tag{4.19}
$$

where $\boldsymbol{\Omega}\in\mathbb{R}^{N_\mathrm{R}\times N_\mathrm{R}}$ is the effective noise power matrix with the elements and given as below

$$
\boldsymbol{\Omega}=\begin{pmatrix}
P_s\sigma_e^2+\sigma_n^2 & P_s\sigma_e^2\rho_{\mathrm{Rx}}^{12} & \cdots & P_s\sigma_e^2\rho_{\mathrm{Rx}}^{1N_\mathrm{T}} \\
 & P_s\sigma_e^2+\sigma_n^2 & \cdots & P_s\sigma_e^2\rho_{\mathrm{Rx}}^{2N_\mathrm{T}} \\
\vdots & \vdots & \ddots & \vdots \\
\cdots & & \cdots & P_s\sigma_e^2+\sigma_n^2
\end{pmatrix},
\tag{4.20}
$$

and $\rho_{\mathrm{Rx}}^{i,j}\ \left(i,j=1,\ldots N_\mathrm{T}\right)$ is the $(i,j)th$ off-diagonal element of the normalized Rx spatial correlation matrix. In Eq. (4.20), the elements in lower triangle are omitted due to the symmetric matrix.

Now is introduction of the singular value decompositions (SVD) for the matrices $\mathbf{Z}$ and $\boldsymbol{\Omega}$ respectively:

$$
\boldsymbol{\Omega}=\mathbf{V}_\omega\boldsymbol{\Lambda}_\omega\mathbf{V}_\omega^H,\ \ \mathbf{Z}=\mathbf{V}_z\boldsymbol{\Lambda}_z\mathbf{V}_z^H,
\tag{4.21}
$$

with nonnegative diagonal singular value matrices $\boldsymbol{\Lambda}_\omega=diag\left(\lambda_1^\omega,\lambda_2^\omega,\ldots,\lambda_{N_\mathrm{R}}^\omega\right)$, and $\boldsymbol{\Lambda}_z=diag\left(\lambda_1^z,\lambda_2^z,\ldots,\lambda_{N_\mathrm{R}}^z\right)$, which containing the eigenvalues arranged in a descending order from top-left to bottom-right. $\mathbf{V}_\omega$, and $\mathbf{V}_z$ the unitary matrices.

By substituting Eq. (4.19), Eq. (4.20) into Eq. (4.17) and applying the matrix inversion lemma [104], yields the lower bound information of the system as follows

$$I_{\text{lb}}^{\text{corr}} = \log_2\left(\left|\mathbf{I}_{N_{\text{R}}} + \mathbf{\Lambda}_{\omega}\Upsilon\mathbf{\Lambda}_{z}\Upsilon^{H}\right|\right) \tag{4.22}$$

with $\Upsilon = \mathbf{V}_{\omega}^{H}\mathbf{V}_{z}$.

From Eq. (4.22), it is clearly noted that when the channel is iid, for example $\mathbf{\Psi}_{\text{R}} = \mathbf{I}_{N_{\text{R}}}$, then Eq. (4.22) becomes Eq. (4.15). If there is no power adaptation, Eq. (4.20) is applied. Furthermore, Eq. (4.22) can be simplified to as follows

$$\begin{aligned} I_{\text{lb}}^{\text{corr}} &= \log_2\left(\left|\mathbf{I}_{N_{\text{R}}} + \mathbf{\Lambda}_{\omega}\Upsilon\mathbf{\Lambda}_{z}\Upsilon^{H}\right|\right) \\ &= \sum_{k=1}^{\nu}\log_2\left(1+\frac{\hat{\lambda}_k}{\hat{\lambda}_k^{\omega}}\hat{p}_k\right) \end{aligned} \tag{4.23}$$

Eq. (4.23) mathematically shows the lower bound on the mutual information of SM-MIMO-ZF system with power adaptation scheme. For the case of $\nu < N_{\text{R}}$, the eigenvalues in $\mathbf{\Lambda}_{\omega}$ are small and dropped due to considering the lower bound. The lower bounds on the channel ergodic capacity are therefore estimated by maximizing the mutual information immediately. In the next section, we analyze the performance of such system under spatial correlation and estimation errors.

4.4 Analysis and Discussion on MIMO Performance in Ergodic Channel Capacity with Spatial Correlation and Estimation Errors

In this section, we present the performance of MIMO systems, which is focused on the channel ergodic capacity; it is of interest to investigate the degradation of the system performance in the non-ideal situation. Here, the instantaneous mutual information uses as a means to estimation the degradation of the MIMO system's performance under influence of spatial correlation coefficient and estimation errors.

We restrict ourselves to the narrowband MIMO and the performance degradation assessments are based on Binary Phase Ship Keying (BPSK) modulation

schemes. The white input signals of power P_s and additive while Gaussian noise with the variance σ_n^2 per receiving antenna.

To evaluate the performance analysis in ergodic capacity of SM-MIMO-ZF systems in the correlated channel, a correlated channel matrix $\mathbf{H}$ is simulated by using a correlation-based channel model, which can be expressed as

$$\mathbf{H} = \mathbf{\Psi}_{\mathrm{R}}^{1/2} \mathbf{H}_{\mathrm{W}} \left(\mathbf{\Psi}_{\mathrm{T}}^{1/2} \right)^{\mathrm{T}} \tag{4.24}$$

where $\mathbf{\Psi}_{\mathrm{R}}$ and $\mathbf{\Psi}_{\mathrm{T}}$ are the normalized correlation matrices at the Rx and Tx respectively, and $\mathbf{H}_{\mathrm{w}} \in \mathbb{C}^{N_{\mathrm{R}} \times N_{\mathrm{T}}}$ contains iid complex Gaussian entries with zero mean and unit variance. Furthermore, due to their simple structures, in the following, consider exponential correlation matrices at the transmitter and the receiver with

$$\mathbf{\Psi}_{\mathrm{T}}(\rho) = \left[\rho_{\mathrm{Tx}}^{|i-j|} \right]_{i,j=1,2,\ldots,n}, \qquad \rho_{\mathrm{Tx}} \in [0,1) \tag{4.25}$$

$$\mathbf{\Psi}_{\mathrm{R}}(\rho) = \left[\rho_{\mathrm{Rx}}^{|i-j|} \right]_{i,j=1,2,\ldots,n}, \qquad \rho_{\mathrm{Rx}} \in [0,1) \tag{4.26}$$

The correlation coefficient at the Rx (or Tx) ranges from 0 to 1 and it is modeled the correlation between two neighboring Rx (or Tx) antennas. With the given channel model, correlation between two antenna elements decreases exponentially with their distance. Again, we strongly focus on the correlation coefficient only at the Rx side.

The Doppler spreads are set as $f_d = 100\mathrm{Hz}$, 400Hz, and 500 Hz, and the normalized feedback delay varied by $99\,\mu\mathrm{s}$, and $600\,\mu\mathrm{s}$, thefore we can obtain the multiplying factors ρ as in Table 4.1.

Table 4.1 The multiplying factor as a function of the Doppler spread and feedback delay

f_d (Hz)	Δt (μs)	ρ
100	99	0.9039
400	600	0.5074
500	600	0.2906

We select the receiver correlation matrix obtained above, i.e. $\Psi_R = \rho \simeq 0.9$, whereas no transmit correlation $\Psi_R = 0$. In the fact that, the correlation coefficients utilized in [8] by measurement campaign where the experiment was conducted in a typical indoor wireless LAN environment with the Tx located along the corridor and the Rx situated in a room with the door opened. The average spatial correlation is about 0.7 at the Rx and 0.8 at the Tx. Finally, the SNR in dB is defined by

$$\gamma_{\text{dB}} = 10 \cdot \log_{10}\left(\frac{\rho \cdot P_s}{\sigma_n^2}\right) = 10 \cdot \log_{10}(\rho \cdot \gamma) \qquad [\text{dB}] \qquad (4.27)$$

Figure 4.4 to Figure 4.8 depict performances on the mutual information (in bps/Hz) versus SNR (in dB) for various MIMO antenna configurations (averaged over 100000 channel realization) in slow-frequency-nonselective uncorrelated and correlated Rayleigh fading channels with the impact of channel estimation errors changing within [0, 1). In general, spatial correlation reduces slightly the ergodic capacity curves from the uncorrelated scenarios, whereas the capacity curve for imperfect CSI at the receiver $\left(\sigma_e^2 = 0.1 \text{ or } 10 \text{ percent and } \sigma_e^2 = 0.5 \text{ or } 50 \text{ percent }\right)$ saturates at the high SNR region, while the capacity for perfect CSI at the receiver $\left(\sigma_e^2 = 0\right)$ continues to increase. On the other hand, at low SNRs, which are out region of interest, the introduction of channel estimation errors shifts slightly the capacity curve to the right with respect to the perfect CSI case.

From these results, it can be demonstrated that the capacity of SM-MIMO system suffers degradation when the CSI is not perfect sufficiently and in spatially correlated signals. Above high SNR values, because of the delay the capacity of the system with CSI at both sides becomes less than the system where CSI is perfectly known at the receiver side only. It can be explained by the fact that when the transmitted power is increased, the power distributed at each channel is increased as well, therefore, more interfered power will be generated.

In terms of SNR performance degradation for practical MIMO systems, the capacity results give the performance degradation (in terms of SNR and/or data rates) between the "best" possible system without CSI errors and the "best" possible system for given level of CSI errors. In contrast, if one considers a specific MIMO system, the performance degradation versus CSI error causes the following two limiting cases. For very high values of SNR $\left(\sigma_n^2 \ll \sigma_e^2\right)$, the channel estimation errors dominate the AWGN noise terms and the BER system performance saturates for increasing SNR values. (A potentially low error floor because of the estimation error will occur). Conversely, for very low SNR values $\left(\sigma_n^2 \gg \sigma_e^2\right)$, the system performance is noise limited, so the CSI error term will result in a minor SNR degradation. Since the channel estimation error causes an additional signal dependent noise term corrupting the signal, a more precise analysis is not elementary and strongly depends on the numerical stability if there are the specific MIMO decoding algorithms [100], [101], and [105].

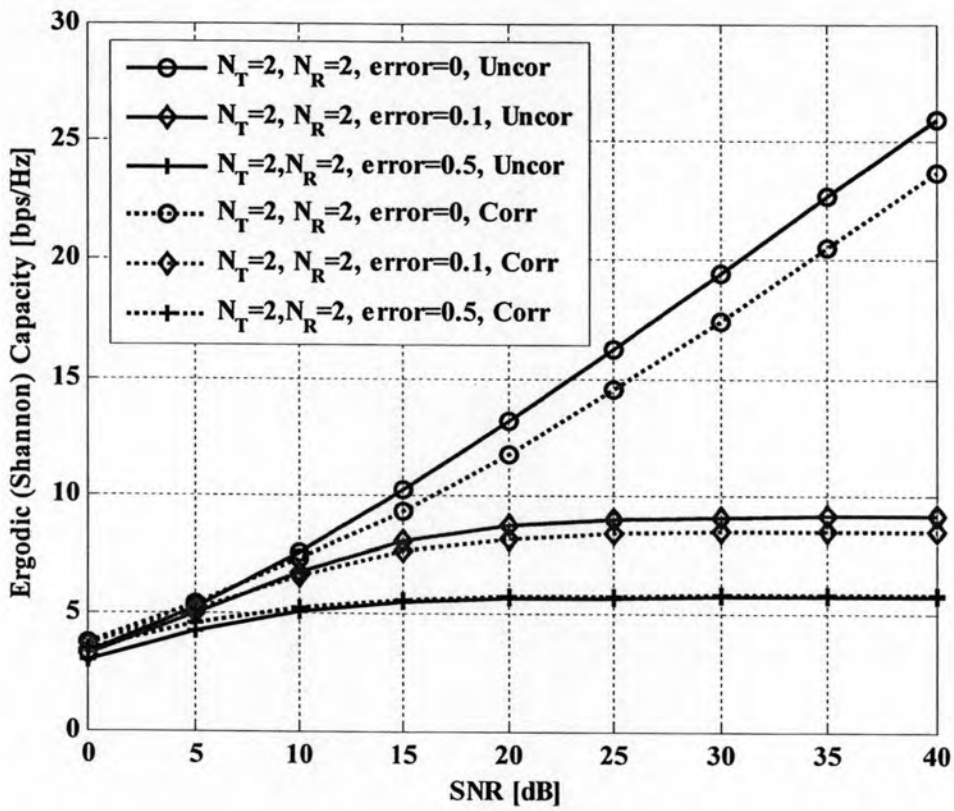

Figure 4.4 Performance on mutual information (in bps/Hz) versus SNR (in dB) for (2x2) MIMO channels with uncorrelated, correlated receiver antennas and estimation errors

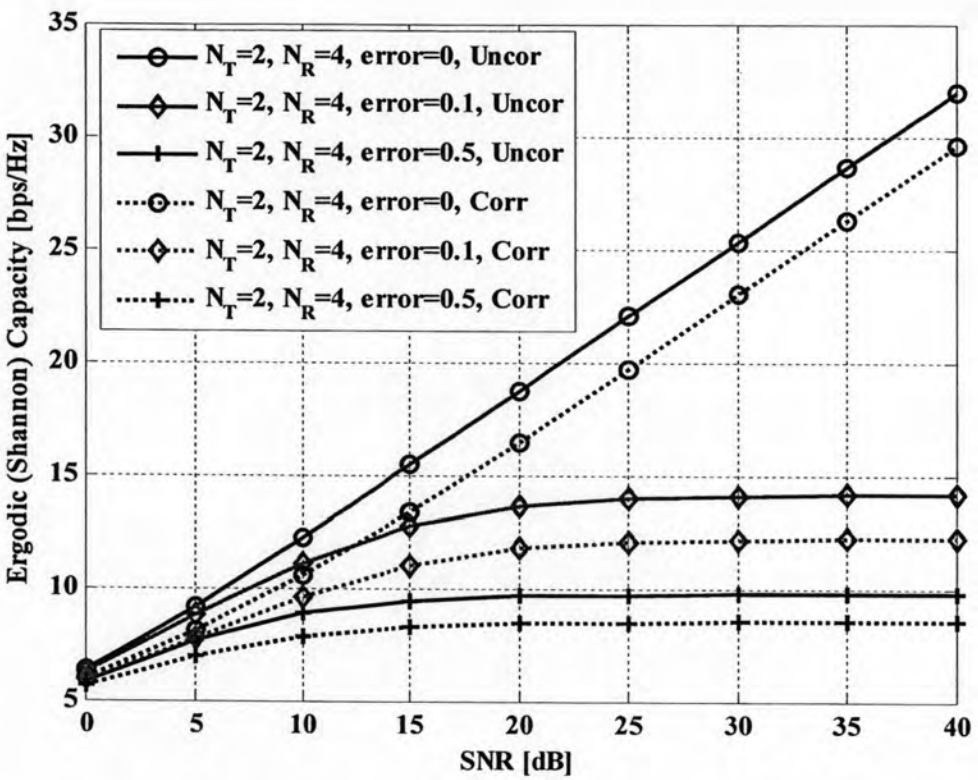

Figure 4.5 Performance on mutual information (in bps/Hz) versus SNR (in dB) for (4x2) MIMO channels with uncorrelated, correlated receiver antennas and estimation errors

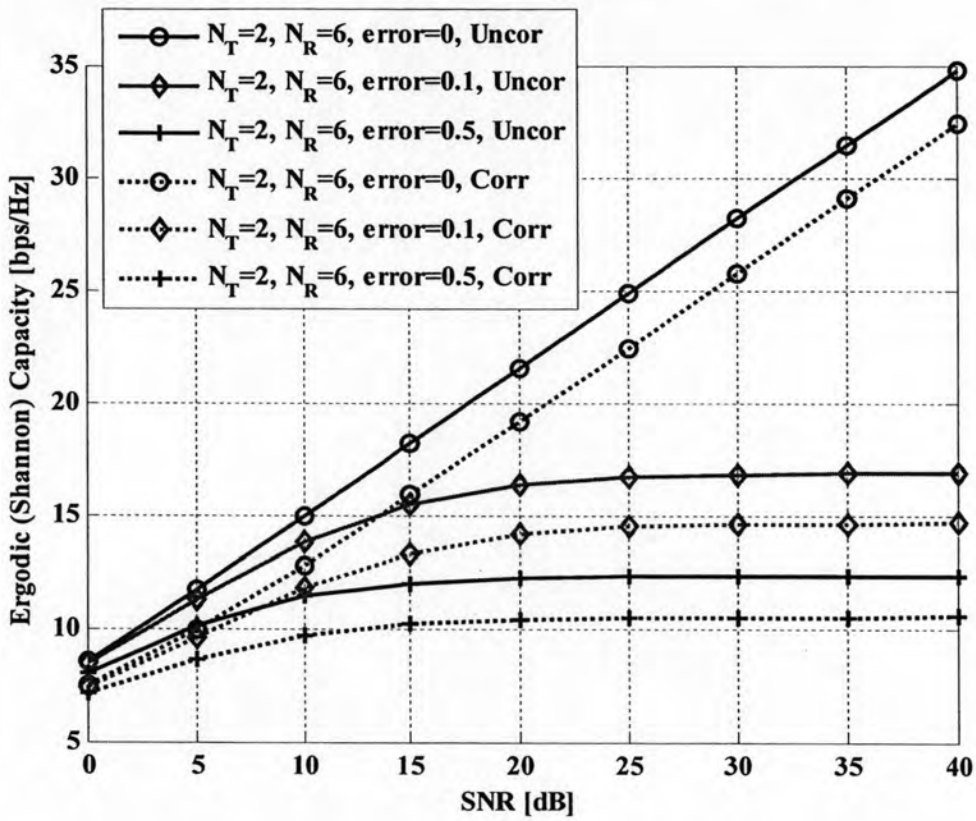

Figure 4.6 Performance on mutual information (in bps/Hz) versus SNR (in dB) for (6x2) MIMO channels with uncorrelated, correlated receiver antennas and estimation errors

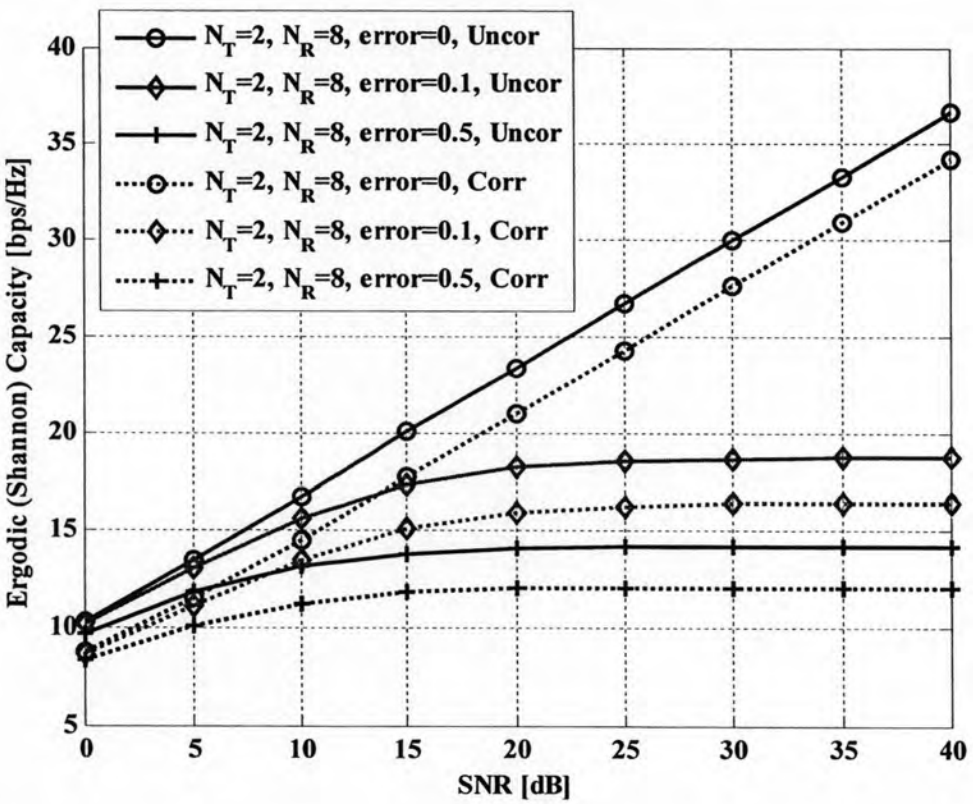

Figure 4.7 Performance on mutual information (in bps/Hz) versus SNR (in dB) for (8x2) MIMO channels with uncorrelated, correlated receiver antennas and estimation errors

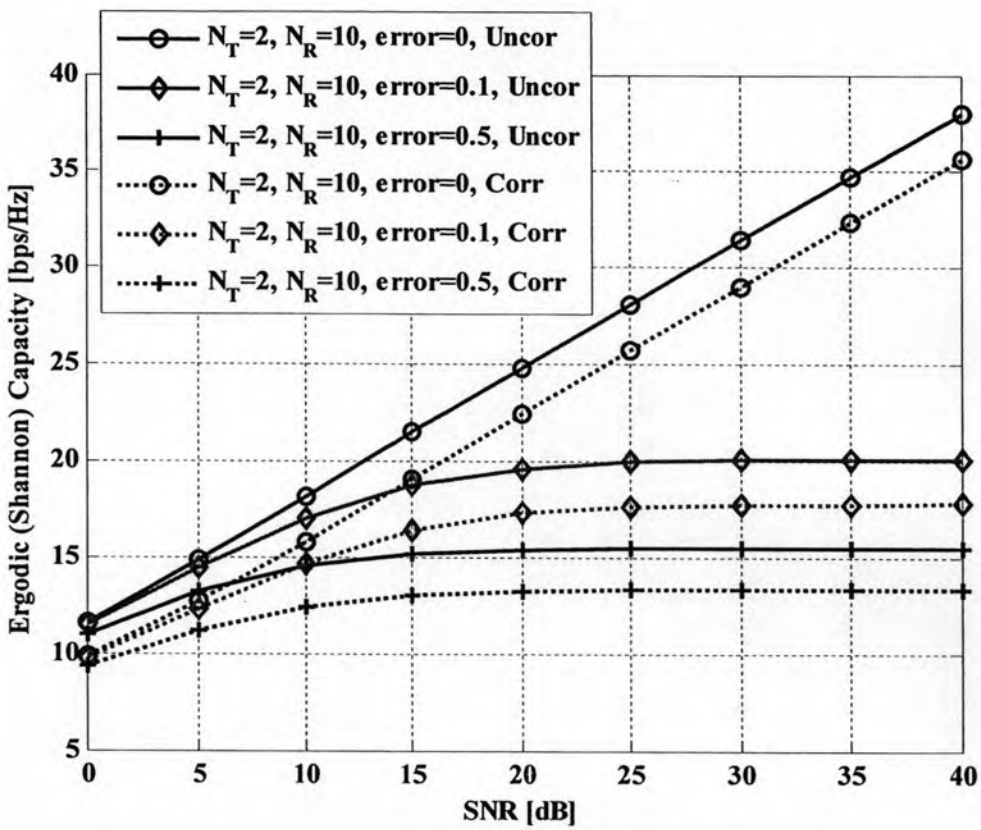

Figure 4.8 Performance on mutual information (in bps/Hz) versus SNR (in dB) for (10x2) MIMO channels with uncorrelated, correlated receiver antennas and estimation errors

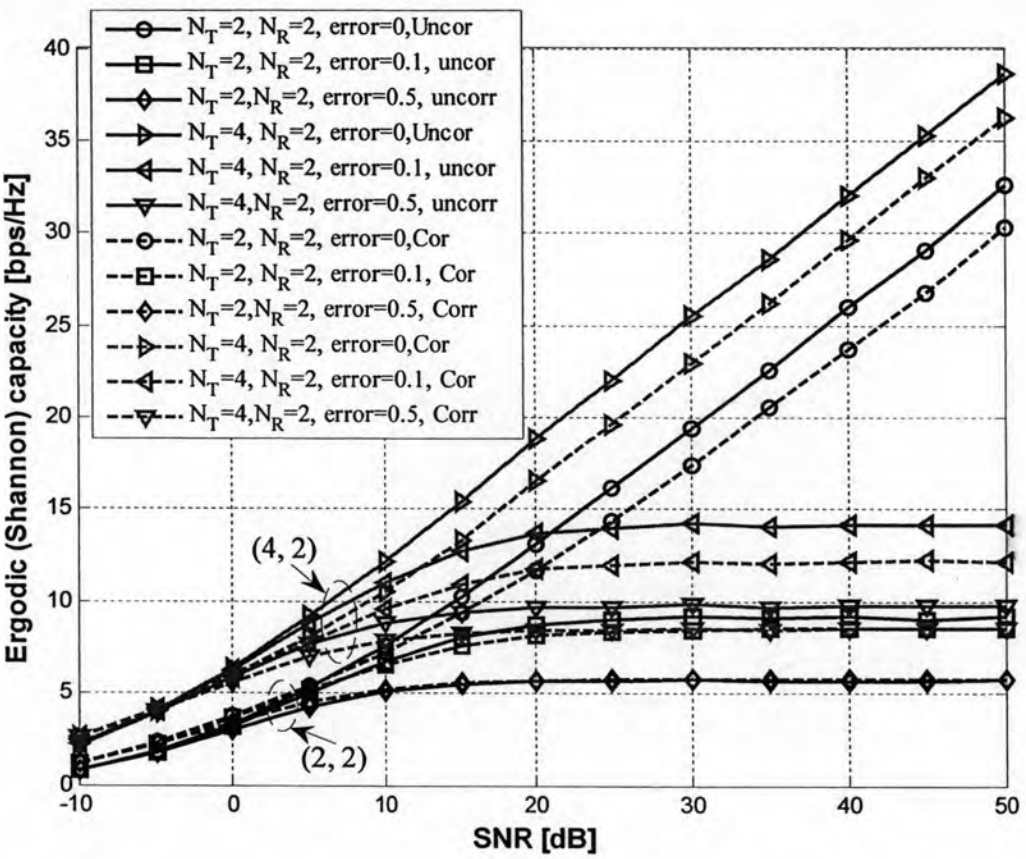

Figure 4.9 Performance comparison on mutual information (in bps/Hz) versus SNR (in dB) for (2x2) and (4x2) MIMO channels with uncorrelated, correlated receiver antennas and estimation errors

4.5 Approximation of BER on the Modulation Schemes: M-PSK and M-QAM

In this Section, the performance of SM-MIMO systems using ZF detector over Rayleigh fading channels will be presented. Much of research on the performance of MIMO systems have been focused on Rayleigh fading channels [106], [107]. Many detectors have been proposed to overcome the effect of the fading and spatial correlation, resulting in a significant gain in system capacity [108]. In [109], the BER performance of the systems in Rayleigh fading channels was evaluated by simulations. The results in that paper provided the signal power from the NLoS components remains the same.

As mentioned in the previous chapter, the data that want to transmit over the wireless propagation channel are digital. The data bits are mapping to signal waveforms that can be transmitted over an (analog) channel. Therefore, digital modulation schemes are choosing in a wireless system, the ultimate goal is to transmit with certain energy as much information as possible over the channel with the certain bandwidth while using a certain transmission quality of BER. Figure 4.10 compares the BER performances of different modulation schemes: M-ary Phase Shift Keying (M-PSK) and M-ary Quadrature Amplitude Modulation (M-QAM).

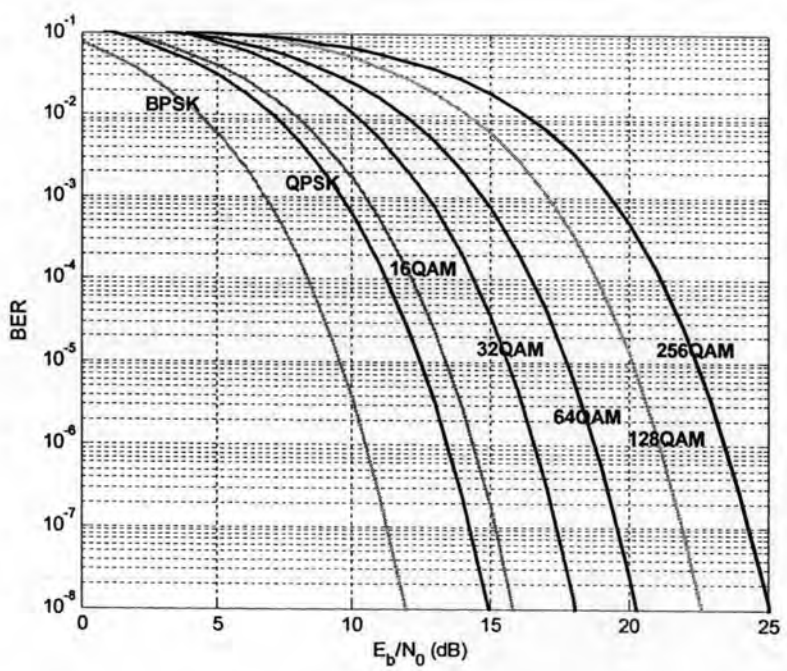

Figure 4.10 Performances of different modulation schemes: M-PSK and M-QAM

The average BER approximations of each substream on the type of modulation either M-PSK or M-QAM with different orders for the SM-MIMO-ZF system in presence of channel estimation errors and feedback delay can be expressed by averaging the instantaneous BER over all SNRs as follows

$$\begin{aligned} \mathrm{BER}_k &= E_{\gamma_k}\left\{\Pr\left(M \mid \gamma_k\right)\right\} \\ &= \int_0^{+\infty} \Pr\left(M \mid \gamma_k\right) f\left(\gamma_k\right) d\gamma_k, \end{aligned} \tag{4.28}$$

where

- $\Pr\left(M \mid \gamma_k\right)$ is the BER conditioned on the γ_k, M is the constellation size, and
- $f\left(\gamma_k\right)$ is the pdf of the *k-th* sub-stream zero-forcing output γ_k and is expressed by [106]

Now we define

$$\mathbf{S} = \mathbf{H}^H \mathbf{H}, \tag{4.29}$$

is always an $N_{\mathrm{R}} \times N_{\mathrm{R}}$ square matrix. It is known that when a complex normally distributed matrix as described is earlier in Chapter 2, the distribution of $\mathbf{S}$ is given by the non-central Wishart distribution [86]. Here we use the notation $\mathbf{S} \sim \widetilde{W}_{N_{\mathrm{T}}}\left(N, \Psi\right)$ to denote a central Wishart distribution, which results when the elements of $\mathbf{H}$ are zero-mean Gaussian random variables, with N degrees of freedom, and is the Hermitian covariance matrix of the columns. The subscript N_{T} explicitly denotes the sample matrix. Also, the notation

$$\mathbf{S} \sim \widetilde{W}_{N_{\mathrm{T}}}\left(N_{\mathrm{R}}, \Psi, \Psi^{-1}\Sigma\Sigma^H\right), \tag{4.30}$$

denotes the non-central Wishart distribution with N_R degrees of freedom, which results when the elements of $\mathbf{H}$ are Gaussian random variables with $\Sigma = \mathrm{E}[\mathbf{H}] \neq 0$.

Here the non-central Wishart distribution is approximated $\mathbf{S} \sim \widetilde{W}_{N_T}(N_R, \Psi, \Psi^{-1}\Sigma\Sigma^H)$ by a central Wishart distribution $\mathbf{S}' \sim \widetilde{W}_{N_T}(N_R, \Psi + (1/N_R)\Sigma^H\Sigma)$ as in [110]. The technique represents a non-central complex Wishart distribution by normal vector. Note that the first order moments of and of approximation are identical. Whereas the second order moment differs by. Hence, this justifies the approximation. In this case, the pdf of the post-processing SNR of each stream is given by

$$f(\gamma_k) = \frac{1}{(\Delta-1)!2^{\Delta}} q_k^{\Delta-1} e^{-\frac{q_k}{2}}, \tag{4.31}$$

where $q_k = \frac{1}{\left[\left(\mathbf{H}^H\mathbf{H}\right)^{-1}\right]_{kk}} > 0$ is a chi-square distributed random variable with $2(N_r - N_t + 1) = 2\Delta$ are degrees of freedom.

The performance of spatial multiplexing with linear detectors is a function of the effective SNR, denoted by γ_k for each stream with $k = 1, 2, \ldots, N_R$, after linear processing at the receiver, the post-detection SNR of the *k*-th stream for the linear ZF equalizer (detector) is expressed as [11]

$$\gamma_k = \frac{\gamma_0}{\left[\left(\mathbf{H}^H\mathbf{H}\right)^{-1}\right]_{kk}^{-1}}, \tag{4.32}$$

where

- $\gamma_0 = \frac{\sigma_x^2}{N_0}$ is the average normalized SNR at each receive antenna,

- $\left[\left(\mathbf{H}^{H}\mathbf{H}\right)^{-1}\right]_{kk}^{-1}$ is the (k, k)-*th* element of matrix $\left(\mathbf{H}^{H}\mathbf{H}\right)^{-1}$.

It is assumed that the (N-1) interferences are Gaussian distributed; the BER of the system by using M-PSK with optimal detection can be expressed by:

$$\mathrm{BER}_k = \frac{2}{\max\left(\log_2 M, 2\right)} \sum_{i=1}^{\min\left(2,\frac{M}{4}\right)} E\left\{ Q\left(\sqrt{\frac{2\left(\lambda+\sigma_e^2\right)\sin^2\frac{(2c-1)\pi}{M}}{\frac{N_{\min}\sigma_n^2}{P_s}+(N_{\min}-1)\sigma_e^2}} \right) \right\} \tag{4.33}$$

with $N_{\min} = \min\left\{N_{\mathrm{T}}, N_{\mathrm{R}}\right\}$.

4.5.1 Case of M-QAM Scheme

For the case of M-QAM, the exact BER expression over AWGN channel is given in [111] by

$$\Pr^{\text{M-QAM}}\left(M \mid \gamma_k\right) \simeq \frac{2}{\sqrt{M}\log_2\sqrt{M}} \sum_{k=1}^{\log_2\sqrt{M}} \sum_{i=1}^{(1-2^{-k})\sqrt{M}-1} \left\{ (-1)^{\left\lfloor \frac{i.2^{k-1}}{M} \right\rfloor} \left(2^{k-1} - \left\lfloor \frac{i.2^{k-1}}{\sqrt{M}} + \frac{1}{2} \right\rfloor \right) \right.$$

$$\left. \times Q\left((2i+1)\sqrt{\frac{3\gamma_k}{(M-1)}} \right) \right\} \tag{4.34}$$

4.5.2 Case of M-PSK Scheme

For the case of M-PSK modulation scheme, the tight BER approximation for M-PSK in AWGN channel is obtained by a simple geometric approach that is based on signal-space concepts in [112] as

$$\Pr^{\text{M-PSK}}\left(M \mid \gamma_k\right) \simeq \frac{2}{\max\left(\log_2 M, 2\right)} \times \sum_{i=1}^{\min\left(2, \left\lceil \frac{M}{4} \right\rceil\right)} Q\left(\sqrt{2\gamma_k} \sin\left(\frac{(2i-1)\pi}{M}\right)\right) \tag{4.35}$$

$\left\lceil \frac{M}{4} \right\rceil$ ceiling operation that presents the smallest integer that is no smaller than $\frac{M}{4}$ and the maximum number of summation terms in Eq. (4.35) is 2 because it is suggested in [112] that the summation of the first 2 terms already provides a very accurate approximation.

In the realistic MIMO channel model under the presence of feedback delay, the ZF estimates the transmitted data vector that can be expressed by

$$\hat{\mathrm{s}}_{\mathrm{ZF}} = \mathbf{G}_{\mathrm{ZF}}\,\mathrm{r} = \hat{\mathbf{H}}^{\dagger}\left(\mathbf{H}\mathbf{F}\mathrm{s} + \mathrm{n}\right) \tag{4.36}$$

where $\hat{\mathbf{H}}^{\dagger}$ is the pseudo-inverse matrix of $\hat{\mathbf{H}}$ of the SM-MIMO-ZF system which can be approximately expressed by [113]

$$\mathbf{G}_{\mathrm{ZF}} = \hat{\mathbf{H}}_t^{\dagger} = \left(\rho\,\mathbf{H}_t + \sqrt{1-\rho^2}\,\mathbf{H}_{t-d} + \mathbf{E}_t\right)^{\dagger} \tag{4.37}$$

Substituting Eq. (4.37) into Eq. (4.36), the received signal vector after ZF processing is

$$\hat{\mathbf{s}}_{ZF}=\frac{1}{\rho}\mathbf{H}^{\dagger}\left[\mathbf{I}_{N_t}-\frac{1}{\rho}\mathbf{H}^{\dagger}\sqrt{1-\rho^2}\mathbf{H}_{\Delta t}-\mathbf{E}\right]\left(\mathbf{HFs}+\mathbf{n}\right)$$

$$=\frac{1}{\rho}\mathbf{Fs}+\frac{1}{\rho}\mathbf{H}^{\dagger}\mathbf{n}-\frac{1}{\rho^2}\left(\mathbf{H}^{\dagger}\mathbf{EFs}+\mathbf{H}^{\dagger}\mathbf{EFn}\right)-$$

$$\frac{\sqrt{1-\rho^2}}{\rho^2}\left(\mathbf{H}^{\dagger}\mathbf{H}_{\Delta t}\mathbf{Fs}+\mathbf{H}^{\dagger}\mathbf{H}_{\Delta t}\mathbf{H}^{\dagger}\mathbf{n}\right) \tag{4.38}$$

$$=\bar{\mathbf{s}}+\bar{\mathbf{n}}$$

where $\bar{\mathbf{s}}$ is the desired signal and $\bar{\mathbf{n}}$ is additional noise plus interference signal, respectively expressed as

$$\bar{\mathbf{s}}=\frac{1}{\rho}\mathbf{Fs}, \tag{4.39}$$

$$\bar{\mathbf{n}}=\frac{1}{\rho}\mathbf{H}^{\dagger}\mathbf{n}-\frac{1}{\rho^2}\left(\mathbf{H}^{\dagger}\mathbf{EFs}+\mathbf{H}^{\dagger}\mathbf{EFn}\right)- \tag{4.40}$$

$$\frac{\sqrt{1-\rho^2}}{\rho^2}\left(\mathbf{H}^{\dagger}\mathbf{H}_{\Delta t}\mathbf{Fs}+\mathbf{H}^{\dagger}\mathbf{H}_{\Delta t}\mathbf{H}^{\dagger}\mathbf{n}\right)$$

Therefore, the zero-forcing processing SNR per symbol of the *k-th* sub-stream can be expressed as

$$\gamma_k=\frac{E\left[\bar{\mathbf{s}}\,\bar{\mathbf{s}}^H\right]}{E\left[\bar{\mathbf{n}}\,\bar{\mathbf{n}}^H\right]}$$

$$=\frac{\rho^2\left[\mathbf{FF}^H\right]_{k,k}}{\rho^2\sigma_n^2+\left(1+\sigma_e^2-\rho^2\right)\left(\mathrm{tr}\left(\mathbf{FF}^H\right)+\sigma_n^2\,\mathrm{tr}\left(\left(\mathbf{H}^H\mathbf{H}\right)^{-1}\right)\right)}\times\frac{1}{\left[\left(\mathbf{H}^H\mathbf{H}\right)^{-1}\right]_{k,k}} \tag{4.41}$$

where we note that $\sigma_e^2=E\left[\mathbf{HH}_{\Delta t}\right]$

Proof (Appendix B)